Determination of Dynamic Tensile Strength of Concrete Using a Split Hopkinson Pressure Bar

ME EN 6960

Nik Benko, John Callaway, Nick Dorsett, Martin Raming

April 25, 2018

Abstract

In this work, the dynamic tensile strength of a brittle concrete material was quantified using a Split Hopkinson Pressure Bar. Pulse shaping and dispersion corrections were used to check stress homogeneity at the specimen interfaces. A Weibull analysis was conducted to determine the shape and scale parameters of the measured data. A Weibull modulus of 5 indicated high variability in fracture strength of the sample population. Measured dynamic strength was higher than quasi-static strength values reported in literature as expected.

1 Introduction

Accurate predictions of material failure are critical to the design of structures and mechanical devices. In order to make useful predictions of failure, material test conditions must replicate real-world loading scenarios as closely as possible. Standard material tests use application-specific test fixtures and specimen geometries to approximate the expected stress state i.e. tension, compression, shear, or combined loading. An additional, and often overlooked, aspect of the loading condition is the rate at which loads are applied. Many structures and devices are designed to be impacted at high enough speeds that the constitutive response of materials is significantly different from the material's quasi-static behavior. In these applications

it is important to quantify a material's failure properties at high strain rates in order to determine if the use of the material is appropriate.

In this report the high strain rate tensile behavior of concrete is investigated. Concrete is a very common material used in large structures such as buildings, bridges, and roadways, all of which may be subject to high strain rate loading. The compressive and tensile strengths of concrete have been shown to increase at high strain rates. The relationship between strain rate and compressive strength is relatively well established, while only few studies have investigated how the tensile strength of concrete changes with loading rate [1]. A thorough understanding of this relationship may be able to further optimize structural design when high rate loading is expected. In order to load the brittle concrete samples in tension, a Flat Brazil Disc specimen is used.

A major challenge in dynamic material testing is accounting for the inertial effects of a rapidly moving loading apparatus. To overcome this challenge, Kolsky adapted a pressure bar technique originally used by Hopkinson to strike thin material specimens at high speeds[2]. The long and thin bars of a Split-Hopkinson Pressure Bar (SHPB), combined with a thin material specimen, allow strain measurements from the bars to be analyzed with one dimensional wave analysis. This simplification of three dimensional mechanics down to a single dimension allows for the inertia of the striker bar to be accounted for.

An unaltered SHPB generates trapezoidal pulses, with sharp leading and trailing edges. This results in high frequency content in the incident pressure wave that creates inaccuracies in strain measurements and may be undesirable for certain material types. The two most common ways of addressing this issue is the use of pulse shaping, as proposed by Frew et al., and dispersion correction, demonstrated by Follansbee [3] [4]. Both methods were used in this investigation. In this report, the experimental apparatus, test protocol, data reduction, and data analysis methods are described in the methods section. A summary of the measured and reduced data is listed in the results section. The relation of these findings to the current literature are then discussed, and final conclusions are drawn.

2 Methods

2.1 Experimental Techniques

2.1.1 Split Hopkinson Pressure Bar

The SHPB system is built off of three main parts: the striker bar, the incident bar, and the transmitted bar as shown in Figure 2 [3] [4] [5]. A gas gun was used to accelerate the striker bar into the incident bar and create a one-dimensional compression wave that travels down the incident bar [5]. Upon reaching a test specimen placed at the end of the bar as in Figure 1, the specimen is deformed at a very high strain rate by the compression wave [6]. This deformation imparts a reaction force into the transmitted bar, creating a new compression wave. The remainder of the energy from the incident wave is reflected back along the incident bar as a tensile wave [7]. The overall wavelength of the incident pulse is twice the length of the striker bar. Therefore, in order to fully measure both the incident and reflected pulses without interference between the two, the incident bar must be at least twice the length of the striker bar. ======= The SHPB system is built off of three main parts: the striker bar, the incident bar, and the transmitted bar as shown in Figure (bar alignment cartoon) [3] [4] [5]. A gas gun was used to accelerate the striker bar into the incident bar and create a one-dimensional compression wave that travels down the incident bar [5]. Upon reaching a test specimen placed at the end of the bar as in Figure 1, the specimen is deformed at a very high strain rate by the compression wave [6]. This deformation imparts a reaction force into the transmitted bar, creating a new compression wave. The remainder of the energy from the incident wave is reflected back along the incident bar as a tensile wave. The overall wavelength of the incident pulse is the length of the striker bar. Therefore, in order to fully measure both the incident and reflected pulses without interference between the two, the incident bar must be at least twice the length of the striker bar.

For a SHPB system to produce valid results, the stress wave must only propagate axially. For this

assumption to hold, several criteria must be met. The bars must be made from a homogeneous, isotropic material and have a uniform cross section, which is achieved through centerless grinding. Finally, striker bar velocity must be kept low enough so that the elastic limit of the incident bar is not reached. It is also assumed that the stress distribution over the cross section of the is uniform [7]. While this is not true in reality, it has been demonstrated that if the length of the bar is at least twenty times the diameter, acceptable results can be obtained [8].

One of the limitations of a SHPB system is that with finite bars, dispersion effects must be considered due to variations in the speed different frequencies travel within a medium [7]. Two methods are commonly used to compensate for dispersion. The first is the use of pulse shaping. Pulse shaping uses a sacrificial material placed between the striker bar and the incident bar. An ideal pulse shaper reduces the initial slope of the incident pulse so that it more closely resembles the specimen material response [3]. By doing this, the high frequency content of the system is decreased and it can be assumed that only a few frequencies dominate the pulse. The second method of compensating for dispersion is through the use of post processing dispersion correction. Measurements are taken by strain gauges in the center of each bar to ensure that the incident and reflected waves are separately recorded [6] [4]. To then march these waveforms forward or backward in time to represent the conditions upon specimen failure, the Fourier series

$$F(n\Delta T) = \frac{A_0}{2} + \sum_{k=1,2,...}^{N} [A_k cos(k\omega_0 n\Delta T - \phi_{TS}) + B_k sin(k\omega_0 n\Delta T - \phi_{TS})] \tag{1}$$

is used, where

$$\begin{aligned} \phi_{TS} &= k\omega_0(\Delta x/C_k) \\ A_0 &= \frac{2}{T}\int_0^T f(x)\,dt \\ A_k &= \frac{2}{T}\int_0^T f(t)cos(k\omega_0 t)\,dt \\ B_k &= \frac{2}{T}\int_0^T f(t)sin(k\omega_0 t)\,dt \end{aligned}$$

Here, T is the period of the wave, ω_0 is the fundamental frequency $\frac{2\pi}{T}$, n = 1,2,...$2N$, where N = half the number of recorded data points, C_k is the speed of a wave at the kth frequency, ΔT is the time step between recording intervals, and Δx is the distance from the strain gauge to the specimen[7]. Once the waves have been propagated so they are at the same point in time, the strain gauge readings can be translated into strain and force values can be determined. Force on the left side of the bar is found through the equation

$$F_1 = A_{Bar} E_{Bar} (\varepsilon_I + \varepsilon_R) \tag{2}$$

and similarly, force on the right side of the bar is

$$F_2 = A_{Bar} E_{Bar} (\varepsilon_T) \tag{3}$$

.

where A_{Bar} is the area of the SHPB, E_{Bar} is the elastic modulus of the SHPB, ε_I, ε_R, and ε_T are the incident, reflected and transmitted strains respectively. From equilibrium both of these force values should be equal . Finally, from ASTM D3957-08 (cite standard) the tensile strength of the Brazil Disc specimens is found from

$$\sigma_t = \frac{2P}{\pi D t} \tag{4}$$

where P is the force applied by one side of the bar, t is the specimen thickness, and D is the specimen diameter. Through the application of forces on the specimen geometry, the compression wave from the SHPB will produce a tensile loading to fail the specimen.

2.1.2 Statistical Analysis

Central tendency and dispersion are two common ways to quantify the distribution of a data set [9]. Central tendency is quantified using the measures of mean and median. The mean of a data set is given by

$$\bar{x} = \sum_{i=1}^{n} \frac{x_i}{n} \tag{5}$$

where $\bar{x}$ is the mean, n is the number of data points and x_i is the ith data point. The median is the central value of an ordered set of the data. Dispersion represents the distribution of data around the central tendency, usually the mean. Dispersion is measured using standard deviation and variance, given by

$$S_x = \left[\sum_{i=1}^{n} \frac{(x_i - \bar{x})^2}{n-1} \right]^{\frac{1}{2}} \tag{6}$$

$$S_x^2 = \sum_{i=1}^{n} \frac{(x_i - \bar{x})^2}{n-1} \tag{7}$$

where S_x is the standard deviation and S_x^2 is the variance.

For experiments involving strength of materials due to brittle fracture, a Weibull distribution function can be applied to show the probability of failure at a given strength value [9]. The Weibull Distribution is given by

$$p(x) = 1 - e^{-\left[\frac{(x-x_o)}{b}\right]^m} \text{ for } x > x_o \tag{8}$$

$$p(x) = 0 \text{ for } x < x_o \tag{9}$$

where $p(x)$ is the probability of failure occurring at x, x_o is the zero strength value of the distribution, b is scale parameter and m is the Weibull slope parameter. The values of distribution parameters x_o, b and m can be determined iteratively or by use of a commercial software such as MATLAB. MATLAB has a built in function, $wblfit.$ that generates the Weibull parameters and probability distribution function with a 95% confidence interval [10].

2.2 Procedure

Concrete Brazil Disc specimens with a diameter of 19.05 mm and thickness of 6.35 mm were loaded in a SHPB. The SHPB utilized 19.05 mm diameter aluminum 7075-T6 bars for the incident and transmitted bars. The incident bar length was 2.438 m and the transmitted bar length was 1.930 m. Aluminum platens with a matching acoustic impedance were attached to the loading end of the incident and transmitted bars

to prevent damage to the SHPB from the concrete specimens. A 1.058 mm thick, 9.525 mm diameter lead pulse shaper was placed on the non-loading end of the incident bar for each test. The striker bar was propelled using a custom gas gun. The experimental setup can be seen in Figure 1.

Initial calibration was conducted to determine a bar wave speed using a gas gun pressure of 10.2 psi. Specimens were tested at varying gas gun pressures, ranging from 8 to 12.5 psi. Strain gauges were arranged in a full bridge configuration to isolate axial strain. Gauges were located 1.219 m from the loading point on the incident bar and 0.965 m from the loading point on the transmitted bar. Voltage outputs from the strain gauges were collected using a Tektronix DPO 2004B oscilloscope and sampled at 125 MHz for a period of 1 ms. No analog or digital filtering was performed.

2.3 Error and Uncertainties

The main source of uncertainty in the experiment was in the data analysis. It has been shown that the data is very sensitive to the exact value of C_0 as well as in shifting the pulse through time [7]. In our data analysis, the wave speed was determined from a calibration experiment. However, force equilibrium was not satisfied, likely due to errors in shifting the incident and/or reflected waves.

Alignment represents two additional potential sources of error. This alignment error could occur either between the different bars or between the specimen and the bar. Although a potential source of error, the trapezoid pulse seen in the calibration test in Figure **??** demonstrates that bar alignment is sufficient. Additionally, even though the stress is not constant over the cross section of the bars, it is assumed to be close enough due to their slenderness.

3 Results and Discussion

The calculation of dynamic tensile strength assumed force homogenization, therefore only the transmitted wave strain was used for analysis. Testing of thirty five concrete Brazil Disc specimens produced a mean dynamic tensile strength of 15.77 MPa, with a median of 15.18 MPa and standard deviation of 3.60 MPa.

A representative voltage trace is shown in Figure 3. Additional data was excluded based on incomplete wave forms captured during the experiment.

The dynamic tensile strength was found to fit previous experimental findings and was significantly larger than the quasi-static tensile strength [1]. Published values for the quasi-static tensile strength of concrete range from 2.2 to 4.2 MPa [11]. This matches previous findings that the tensile strength of concrete increases with increased strain rate [1] [12]. Additionally, the data was also found to fit a Weibull distribution with $x_o = 7.84$ MPa, $b = 17.18$ MPa and $m = 4.9951$. A Weibull Probability Distribution Function plot was created to verify the Weibull distribution parameters and is presented in Figure 4. A comparison of the gas gun pressure and dynamic tensile strength of concrete showed no significant relationship, which is visualized in Figure 5.

The pulse shaper as mentioned previously was chosen based on the lower rise of the generated pulse when compared to pulses created using other pulse shapers as shown in Figure 6. By using a pulse shaper a value of 50 was used for k instead of f_N as suggested by Li and Lambros [13] to aid in computation time with out loss of accuracy.

4 Conclusion

For this report, dynamic evaluation of concrete tensile strength was performed. The previously reported positive correlation between strain rate and ultimate tensile strength was confirmed. However, little correlation between SHPB gas gun pressure was observed. Future examinations of the dynamic behavior of material may wish to additionally measure striker bar velocity in order to further quantify the effects of gas gun pressure. A Weibull analysis of the sample distribution showed moderate variance in strength within the sample.

5 Figures

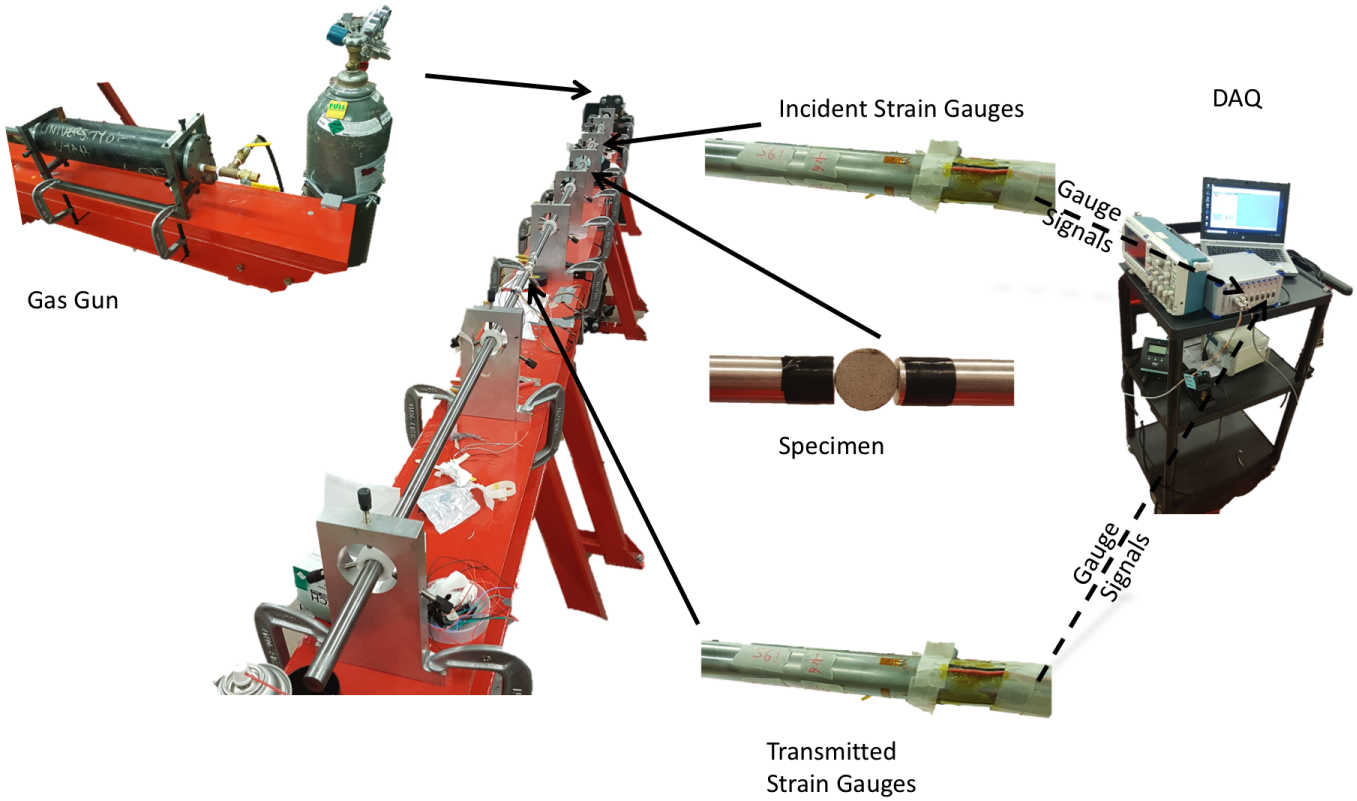

Figure 1: Experimental setup of the Split Hopkinson Pressure Bar

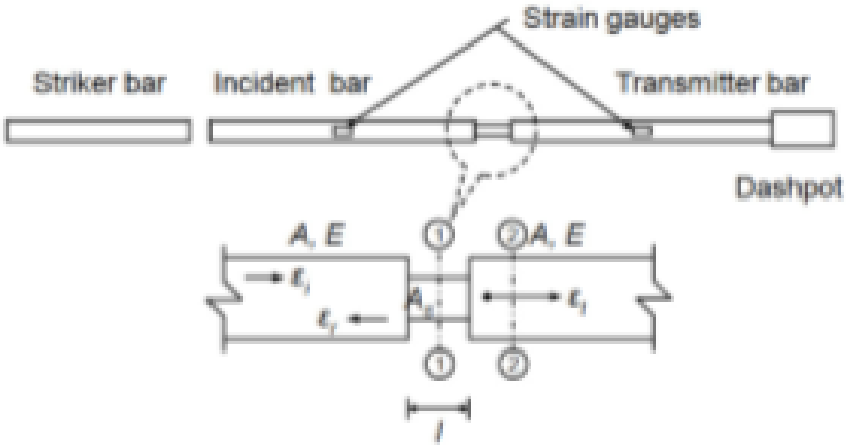

Figure 2: Diagram of the bar alignment and configuration in a SHPB system [14]

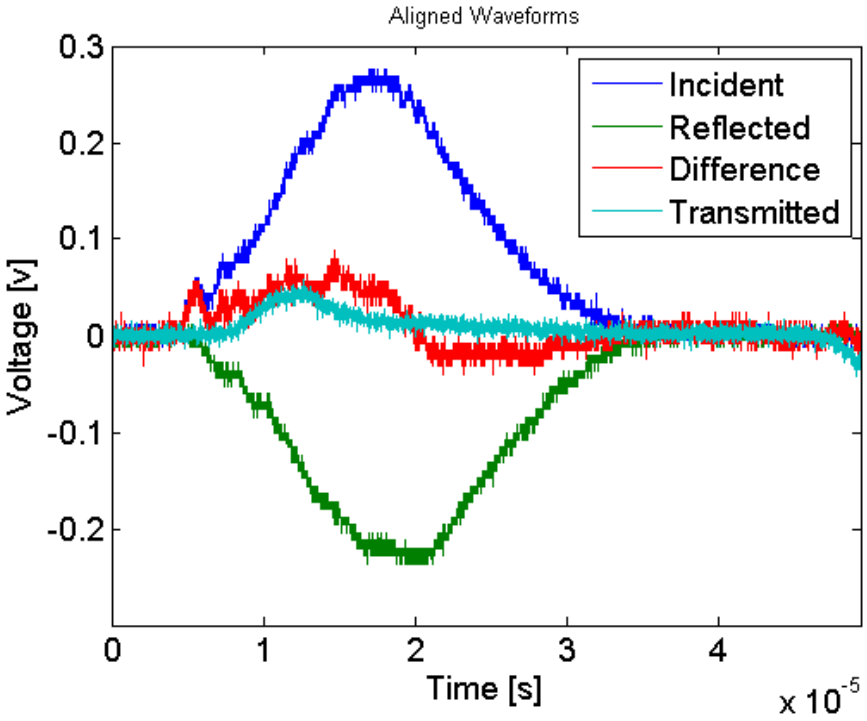

Figure 3: Sample trace of aligned waveforms. Difference between incident and reflected wave is compared to measured transmitted wave

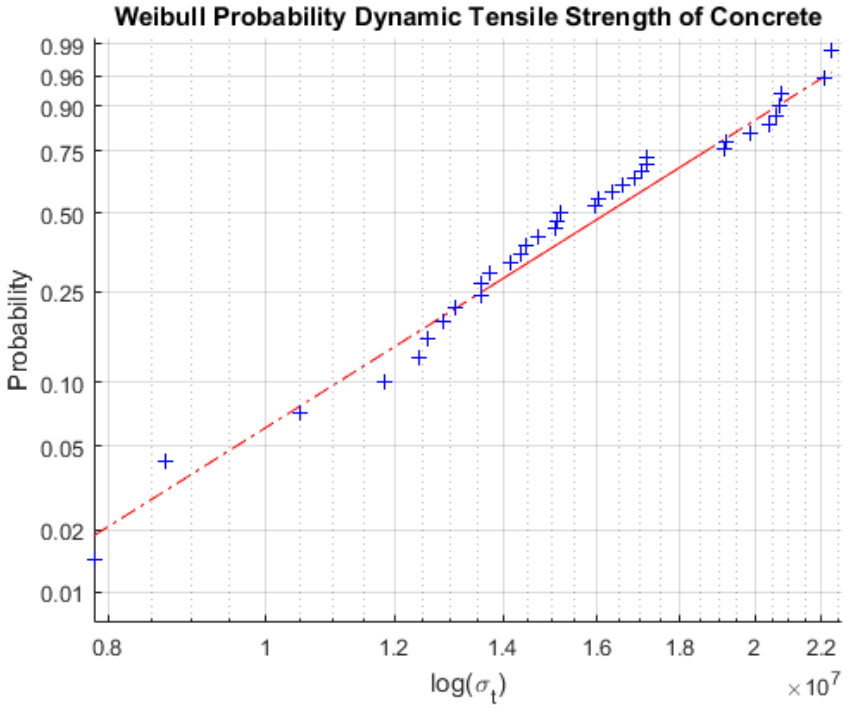

Figure 4: Weibull Probability Distribution Function plot of concrete Brazil Disc specimens

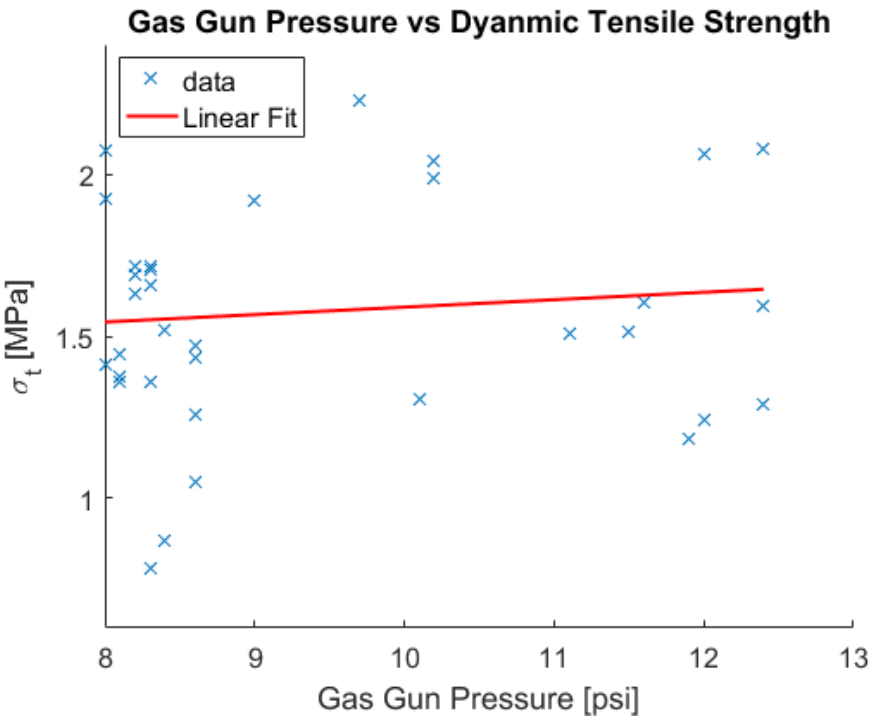

Figure 5: Comparison of Gas Gun Pressure and Calculated Dynamic Tensile Strength of Concrete

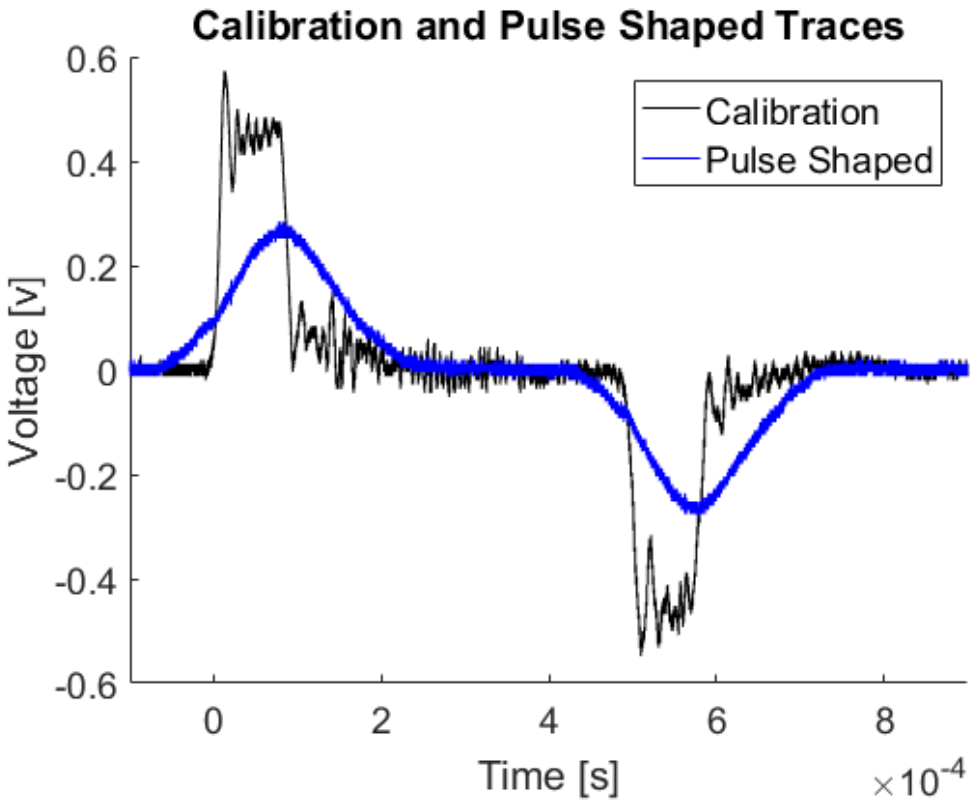

Figure 6: Calibration wave form and comparison of the waveforms generated by use of different pule shapers with the bars apart.

References

[1] X. Jin, C. Hou, X. Fan, C. Lu, H. Yang, X. Shu, and Z. Wang, "Quasi-static and dynamic experimental studies on the tensile strength and failure pattern of concrete and mortar discs," in *Scientific Reports*, 2017.

[2] H. Kolsky, "An investigation of the mechanical properties of materials at very high stain rates of loadin," *Proc. Royal Soc.*, 1949.

[3] W. C. D.J. Frew, M. J. Forrestal, "Pulse shaping techniques for testing brittle materials with a split hopkinson pressure bar," *Experimantal Mechincs*, vol. 42, pp. 93–106, 2002.

[4] C. F. P.S. Follansbee, "Wave propagation in the split hopkinson pressure bar," *Tansactions of the ASME*, vol. 105, pp. 93–106, 1983.

[5] W. C. D.J. Frew, M. J. Forrestal, "A split hopkinson pressure bar technique to determine compresive stress-strain data for rock materials," *Experimantal Mechincs*, vol. 41, pp. 40–46, 2001.

[6] K. X. Z. T. F. Dai, S. Huang, "Some fundemental issues in dynamic compresion and tension test of rocks using split hopkinson pressure bar," *Rock Meck Rock Eng*, 2010.

[7] J. W. G. J. Bazle A. Gama, Sergey L. Lopatnikov, "Hopkinson bar experimental technique: A critical review," *Applied Mechanics*, 2004.

[8] R. Davies, "A critical study of the hopkinson pressure bar," *IEEE*, 1948.

[9] J. W. D. Arun Shukla, *Experimental Solid Mechanics*.

[10] M. Inc, "Matlab and statistics toolbox release 2016b."

[11] D. M. S U Pillai, *Reinforced Concrete Design, Third Edition*.

[12] M. Z. D.L. Grote, S.W. Park, "Dynamic behavior of concreate at high strain rates and pressures: I. expermintal characterization," *Impact Engineering*, 2001.

[13] J. L. Z. Li, "Determination of dynamic response of brittle composites by the use of the split hopkinson pressure bar," *Composites Science and Technology*, 1999.

[14] A. S. J. Ozbolt, J. Weerheijm, "Dynamic tensile resistance of concrete - split hopkinson bar test," *IEEE*.